

KCL-PH-TH/2015-19, LCTS/2015-09, CERN-PH-TH/2015-085

Not only are perturbative QCD calculations doing a fantastic job overall of predicting the production cross sections for jets and massive vector bosons, but also for the Higgs boson. Accurate higher-order QCD calcula-

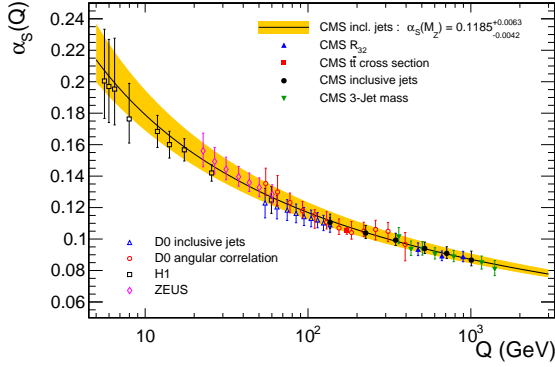


Figure 2: Jet production measurements at the LHC show that  $\alpha_s$  continues to run downward at energies beyond 1 TeV [3].

tions are at a premium for the dominant gluon-fusion contribution to the Higgs production cross section. Several different NNLO calculations are available, and are included in various publicly-available tools [4]. Unfortunately, the agreement between them is not yet perfect. Fortunately, progress is being made on NNNLO calculations [5]. These will improve the theoretical accuracy, but progress in convergence between the parton distribution functions will also be needed in order to reduce the theoretical uncertainties below the experimental measurement uncertainties.

### 3. Flavour Physics

Another pillar of the SM is the Cabibbo-Kobayashi-Maskawa (CKM) model of flavour mixing and CP violation. It is in general very successful, as seen in Fig. 3 [6]. For example, the second-greatest discovery during Run 1 of the LHC was perhaps the measurement by the CMS and LHCb Collaborations of the rare decay  $B_s \rightarrow \mu^+ \mu^-$ , with a branching ratio in good agreement with the SM prediction [7]:

$$BR(B_s \rightarrow \mu^+ \mu^-) = 2.8_{-0.6}^{+0.7} \times 10^{-9}, \quad (1)$$

as seen in Fig. 4. However, the joint CMS and LHCb analysis [7] also has an suggestion of a  $B_d \rightarrow \mu^+ \mu^-$  signal that is larger than the SM prediction:

$$BR(B_d \rightarrow \mu^+ \mu^-) = 3.9_{-1.4}^{+1.6} \times 10^{-10}, \quad (2)$$

as also seen in Fig. 4. If confirmed, this measurement would conflict not just with the SM, but also models with minimal flavour violation (MFV), including many supersymmetric scenarios. Something to watch during Run 2!

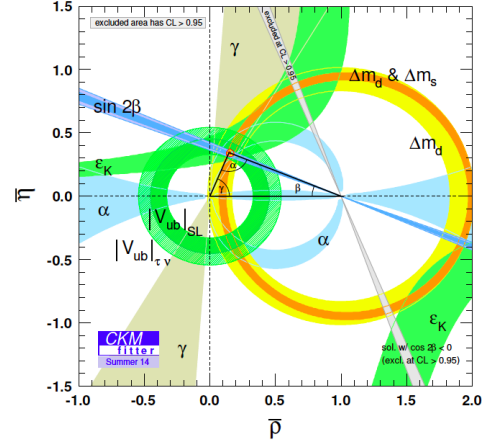


Figure 3: Flavour and CP violation measurements generally agree well with the CKM paradigm [6].

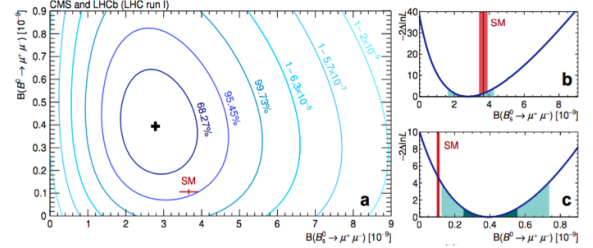


Figure 4: **a:** Measurements by the CMS and LHCb Collaborations of  $B_{s,d} \rightarrow \mu^+ \mu^-$  decays, including **b** a clear signal for  $B_s \rightarrow \mu^+ \mu^-$  decay that agrees with the SM, and **c** a hint of  $B_d \rightarrow \mu^+ \mu^-$  decay, possibly at a rate larger than expected in the SM [7].

There is scope elsewhere for deviations from CKM predictions: for example, the data allow an important contribution to  $B_s$  meson mixing from physics beyond the SM (BSM) [6]. Also, there are issues with  $e - \mu$  universality in semileptonic  $B$  decays [8] and a persistent anomaly in the  $P'_5$  angular distribution for  $B^0 \rightarrow K^{*0} \mu^+ \mu^-$  [9]. Could this be related to the intriguing excess in  $H \rightarrow \mu \tau$  decay reported by the CMS Collaboration [10], which is discussed later? Other points to watch include discrepancies in the determinations of the  $V_{ub}$  CKM matrix element and the Tevatron diimuon asymmetry anomaly [11]. However, some anomalies do seem to be going away, such as the branching ratio for  $B_u \rightarrow \tau^+ \nu$  decay, which is now in good agreement with the SM [12] and the forward-backward asymmetry in  $t\bar{t}$  production [13], which is consistent with the latest higher-order QCD calculations [14], as is the  $t\bar{t}$  rapidity asymmetry measured at the LHC. However, there are still plenty of flavour physics issues to be addressed during LHC Run 2.

## 4. Higgs Physics

The Higgs boson may be regarded as, on the one hand, the capstone of the glorious arch of the SM or, on the other hand, as the portal giving access to new physics. In this Section we discuss first the extent to which the new particle discovered on July 4th, 2012 fulfils its SM rôle, and then what hints it may be able to provide about possible BSM physics.

### 4.1. Mass Measurements

The mass of the Higgs boson is measured most accurately in the  $\gamma\gamma$  and  $ZZ^* \rightarrow 2\ell^+2\ell^-$  final states, and ATLAS and CMS have both reported accurate measurements in each of these final states as shown in Fig. 5. ATLAS measures [15]

$$\begin{aligned} H \rightarrow \gamma\gamma : m_H &= 126.02 \pm 0.51 \text{ GeV}, \\ H \rightarrow ZZ^* : m_H &= 124.51 \pm 0.52 \text{ GeV}, \end{aligned} \quad (3)$$

and CMS measures [16]

$$\begin{aligned} H \rightarrow \gamma\gamma : m_H &= 124.70 \pm 0.34 \text{ GeV}, \\ H \rightarrow ZZ^* : m_H &= 125.59 \pm 0.45 \text{ GeV}. \end{aligned} \quad (4)$$

Combining all these measurements, the ATLAS and CMS Collaborations find [17]

$$m_H = 125.09 \pm 0.24 \text{ GeV}. \quad (5)$$

In addition to being a fundamental measurement in its own right, and casting light on the possible validity of various BSM models (for example, this value is perfectly consistent with supersymmetric predictions [18]), the precise value of  $m_H$  is also important for the stability of the electroweak vacuum in the Standard Model [19], as discussed later.

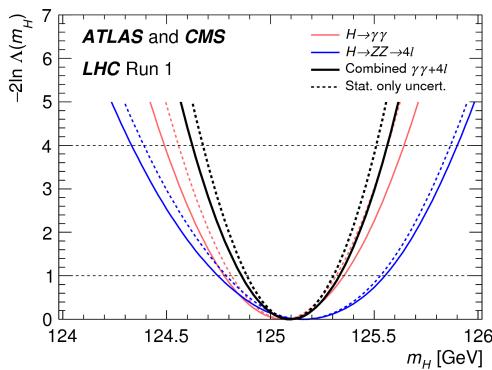


Figure 5: Measurements of  $m_H$  by ATLAS and CMS in the  $\gamma\gamma$  and  $ZZ^* \rightarrow 2\ell^+2\ell^-$  final states, as compiled in [17].

### 4.2. The Higgs Spin and Parity

The fact that the Higgs boson decays into  $\gamma\gamma$  excludes spin 1, and spin 0 is expected, but spins 2 and higher are also possible in principle. The Higgs spin has been probed in many ways [20, 21, 22], via its production and decay rates [23], the kinematics of Higgs production in association with the  $W^\pm$  and  $Z^0$  [24], and decay angular distributions for  $W^+W^-$ ,  $ZZ$  and  $\gamma\gamma$  final states [25]. The results of tests using the kinematics of associated  $H + W^\pm/Z^0$  production at the Tevatron are shown in Fig. 6 [22]. By now there is overwhelming evidence against the Higgs boson having spin 2. Moreover, as also seen in Fig. 6 [22], it has been established that its couplings to  $W^+W^-$  and  $ZZ$  are predominantly CP-even, i.e., it couples mainly as a scalar, not as a pseudoscalar.

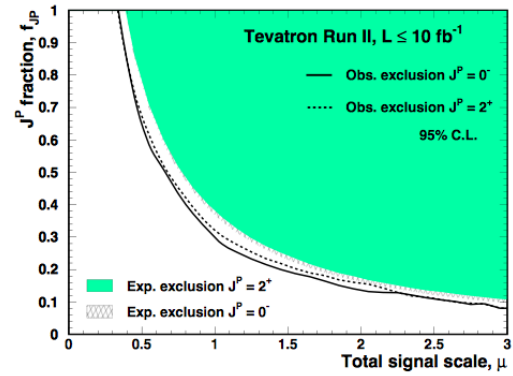


Figure 6: Tests of spin-parity hypotheses for the Higgs boson via the kinematics of associated  $H + W^\pm/Z^0$  production at the Tevatron [22].

### 4.3. Higgs Couplings

As seen in Fig. 7, the strengths of the Higgs signals measured by ATLAS in individual channels [26] are generally compatible with the SM predictions (as are CMS measurements [27]) within the statistical fluctuations, which are inevitably large at this stage. ATLAS and CMS report the following overall signal strengths after combining their measurements in the  $\gamma\gamma$ ,  $ZZ^*$ ,  $WW^*$ ,  $b\bar{b}$  and  $\tau^+\tau^-$  channels:

$$\begin{aligned} \text{ATLAS} : \mu &= 1.30 \pm 0.12 \pm 0.10 \pm 0.09, \\ \text{CMS} : \mu &= 1.00 \pm 0.09^{+0.08}_{-0.07} \pm 0.07. \end{aligned} \quad (6)$$

Both averages are quite compatible with the SM and with each other, as is also true of the Tevatron measurements [28].

Because of its connection to mass generation, the couplings of the Higgs boson to other particles in the SM should be related to their masses: linearly for

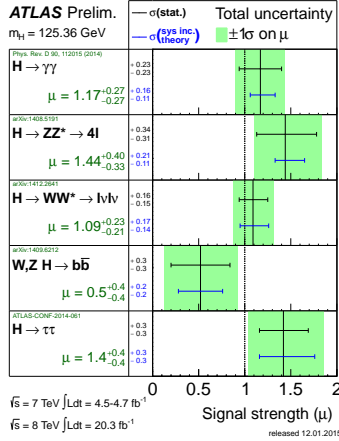


Figure 7: The Higgs signal strengths  $\mu$ , normalised to unity for the SM, as measured by ATLAS [26].

fermions, quadratically for bosons, and be scaled by the Higgs vev  $v = 246$  GeV. These predictions are implicit in the measurements in Fig. 7, and are tested directly in Fig. 8. The latter displays a global fit in which the Higgs coupling data are parametrised as [29]

$$\lambda_f = \sqrt{2} \left( \frac{m_f}{M} \right)^{(1+\epsilon)}, \quad g_V = 2 \left( \frac{M_V^{2(1+\epsilon)}}{M^{(1+\epsilon)}} \right). \quad (7)$$

As seen in the left panel of Fig. 8, the data yield

$$\epsilon = -0.022^{+0.020}_{-0.043}, \quad M = 244^{+20}_{-10} \text{ GeV}, \quad (8)$$

which is in excellent agreement with the SM predictions  $\epsilon = 0$ ,  $M = 246$  GeV. Similar results have also been found recently in an analysis by the CMS Collaboration [27]. It seems that Higgs couplings indeed have the expected characteristic dependence on particle masses.

According to the SM, flavour should be conserved to a very good approximation in Higgs couplings to fermions. This is consistent with the available upper limits on low-energy effective flavour-changing interactions, which would, however, also allow lepton-flavour-violating Higgs couplings that are much larger than the SM predictions [30]. Looking for such interactions is therefore a possible window on BSM physics. On the basis of low-energy data, we estimated that the branching ratios for  $H \rightarrow \mu\tau$  and  $H \rightarrow e\tau$  decays could each be as large as  $O(10)\%$ , i.e., as large as  $\text{BR}(H \rightarrow \tau\tau)$ , whereas the branching ratio for  $H \rightarrow \mu e$  could only be much smaller,  $\lesssim 10^{-5}$  [30]. The CMS Collaboration has recently reported a measurement [10]

$$\text{BR}(H \rightarrow \mu\tau) = 0.89^{+0.40}_{-0.37} \%, \quad (9)$$

which is  $\sim 2.5\sigma$  different from zero. SM flavour physics predictions are therefore being probed more stringently

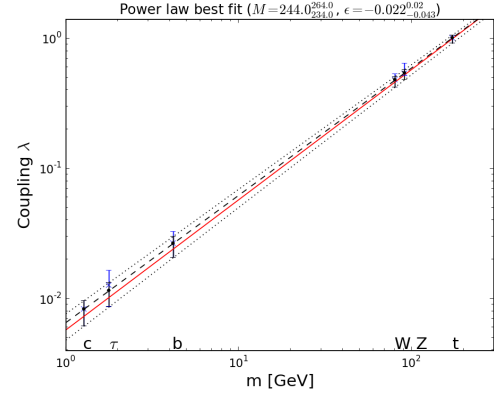


Figure 8: A global fit to the  $H$  couplings of the form (7) (central values as dashed and  $\pm 1\sigma$  values as dotted lines), which is very consistent with the linear mass dependence for fermions and quadratic mass dependence for bosons (solid red line) expected in the SM [29].

by the LHC than by low-energy experiments, and we are keen to see corresponding results from ATLAS and from Run 2 of the LHC!

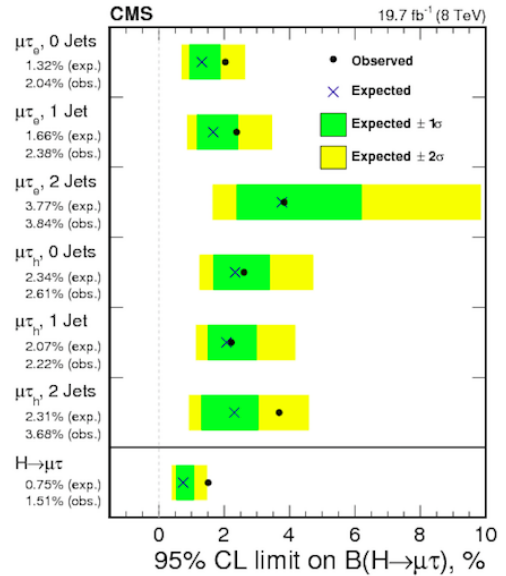


Figure 9: Results from the CMS search for  $H \rightarrow \mu\tau$  decay [10].

Although all the indications are that the dominant Higgs couplings are CP-even, as seen, e.g., in Fig. 6 above, there may also be an admixture of CP-odd couplings, whose fraction may depend on the particle whose coupling to the Higgs boson are being probed. Since the leading CP-odd  $H$  coupling to fermions would have the *same* (zero) dimension as the leading CP-even coupling, whereas the leading CP-odd  $H$  coupling to

massive vector bosons would have *higher* dimension than the leading CP-even coupling, the latter may be more suppressed. Ideas for probing CP violation in  $H \rightarrow \tau^+\tau^-$  decay have been suggested [31], and CP violation may also be probed in the  $Ht\bar{t}$  couplings [32]. As seen in Fig. 10, this could affect the total cross sections for associated  $Ht\bar{t}$ ,  $Ht$  and  $H\bar{t}$  production, shown as functions of  $\zeta_t \equiv \arctan(\text{CP-odd coupling}/\text{CP-even coupling})$ . If  $\zeta_t \neq 0$ , a CP-violating transverse polarization asymmetry is in principle observable in  $Ht$  and  $H\bar{t}$  production, as discussed in [32].

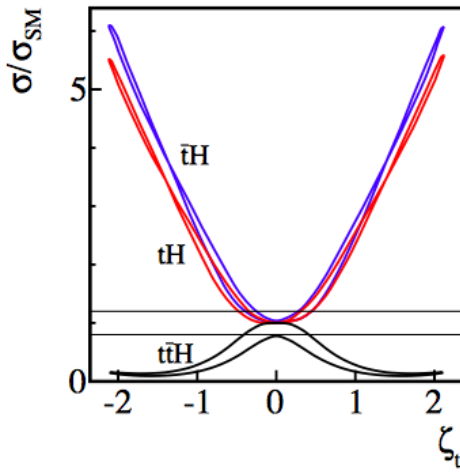


Figure 10: The effects of a CP-violating coupling on the  $Ht\bar{t}$ ,  $Ht$  and  $H\bar{t}$  production cross sections, taking into account the current constraints from the  $Hgg$  and  $H\gamma\gamma$  couplings [32].

#### 4.4. Is the Higgs Boson Elementary or Composite?

One of the key questions about the Higgs boson is whether it is elementary or composite. One might have thought that a composite Higgs boson would naturally have a mass comparable to the scale of compositeness, but the mass can be suppressed if it is a pseudo-Nambu-Goldstone boson with a mass that is protected by some approximate symmetry, perhaps becoming consistent with the measured Higgs mass  $\sim 125$  GeV. This possibility may be probed using a phenomenological Lagrangian  $\mathcal{L}$  with free  $H$  couplings, that may be constrained using  $H$  decay and production data. Since the Standard Model relation  $\rho \equiv m_W/m_Z \cos \theta_W = 1$  agrees well with the data, one usually assumes that the phenomenological Lagrangian has a custodial symmetry:  $SU(2) \times SU(2) \rightarrow SU(2)$ . Then one may parametrise the leading-order terms in  $\mathcal{L}$  as follows:

$$\mathcal{L} = \frac{v^2}{4} \text{Tr} D_\mu \Sigma^\dagger D^\mu \Sigma \left( 1 + 2a \frac{H}{v} + b \frac{H^2}{v^2} + \dots \right)$$

$$\begin{aligned} & - \bar{\psi}_L \Sigma \left( 1 + c \frac{H}{v} + \dots \right) \\ & + \frac{1}{2} (\partial_\mu H)^2 + \frac{1}{2} m_H^2 H^2 + d_3 \frac{1}{6} \left( \frac{3m_H^2}{v} \right) H^3 \\ & + d_4 \frac{1}{24} \left( \frac{3m_H^2}{v} \right) H^4 + \dots, \end{aligned} \quad (10)$$

where

$$\Sigma \equiv \exp \left( i \frac{\sigma^a \pi^a}{v} \right). \quad (11)$$

The free coefficients  $a, b, c, d_3$  and  $d_4$  are all normalised so that they are unity in the SM, and one searches for observable deviations from these values that could be signatures of composite models.

Fig. 11 shows one such analysis [29], that looked for possible rescalings of the  $H$  couplings to bosons by a factor  $a$  and to fermions by a factor  $c$ <sup>1</sup>. Fig. 11 shows no sign of any deviation from the SM predictions  $a = c = 1$ . The yellow lines in Fig. 11 show the predictions of specific composite models that are excluded unless (in some cases) their predictions are adjusted to resemble those of the SM.

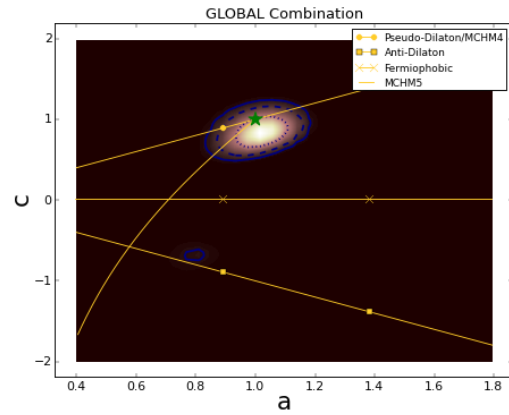


Figure 11: A global fit to bosonic and fermionic  $H$  couplings rescaled by factors  $a$  and  $c$ , respectively. The SM prediction  $a = c = 1$  is shown as the green star [29], and the yellow lines show the possible predictions of some composite models.

Since the properties of the Higgs boson as well as other particles continue to agree with the SM, it is increasingly popular approach to regard the SM as an effective field theory (EFT) valid at low energies

<sup>1</sup>For a similar recent result from the CMS Collaboration, see [16]. The Higgs Cross Section Working group defines the quantities  $\kappa_V \equiv a$  and  $\kappa_f \equiv c$  [4], which are used by ATLAS and CMS.



$< 1$  TeV. The effects of BSM physics at higher scales may then be parametrised via higher-dimensional EFT operators constructed out of SM fields, as a first approximation, with coefficients that can be constrained by precision electroweak data, Higgs data and triple-gauge couplings (TGCs).

Ref. [33] discusses the operators entering electroweak precision tests (EWPTs) at LEP, together with 95% CL bounds on their individual coefficients when they are switched on one at a time, and also when marginalised in a simultaneous global fit. Results for the EFT coefficients  $\bar{c}_{LL}^{(3)l}$ ,  $\bar{c}_T$ ,  $\bar{c}_W + \bar{c}_B$  and  $\bar{c}_R^e$ , which affect the leptonic observables  $\{\Gamma_Z, \sigma_{\text{had}}^0, R_e^0, R_\mu^0, R_\tau^0, A_{\text{FB}}^{0,e}, m_W\}$ , and the EFT coefficients  $\bar{c}_L^q$ ,  $\bar{c}_L^{(3)q}$ ,  $\bar{c}_R^u$  and  $\bar{c}_R^d$ , which contribute to the hadronic observables  $\{R_b^0, R_c^0, A_{\text{FB}}^{0,b}, A_{\text{FB}}^{0,c}, A_b, A_c\}$ , are shown in Fig. 12. The upper (green) bars show the ranges for each of EFT coefficient when it is varied individually, assuming that the other EFT coefficients vanish, and the lower (red) bars show the ranges for a global fit in which all the EFT coefficients are allowed to vary simultaneously, neglecting any possible correlations. The ranges of the coefficients are translated in the legend at the top of the left panel of Fig. 12 into ranges of a large mass scale  $\Lambda$ . All the sensitivities are in the multi-TeV range.

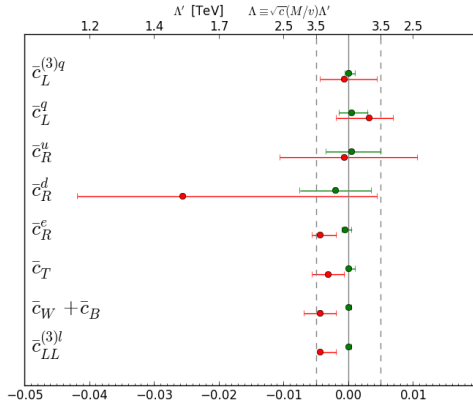


Figure 12: The 95% CL ranges found in analyses of the leptonic and hadronic LEP observables. The upper (green) bars denote single-coefficient fits, and the lower (red) bars denote marginalised multi-coefficient fits. The upper-axis should be read  $\times \frac{m_W}{v} \sim 1/3$  for  $\bar{c}_W + \bar{c}_B$ . [33]

Other operators contribute to Higgs physics and TGCs, and important information on possible values of their coefficients is provided by kinematic distributions [34], as well as by total rates, as illustrated in Fig. 13.

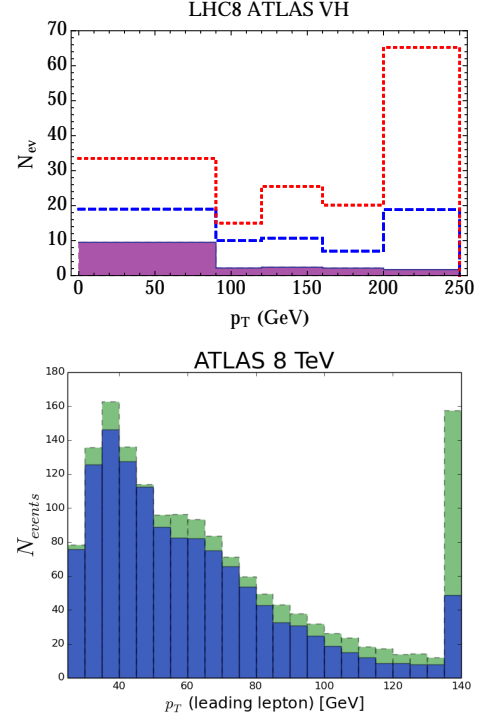


Figure 13: Upper panel: Simulation of the  $p_T^V$  distribution in  $(V \rightarrow 2\ell) + (H \rightarrow b\bar{b})$  events at the LHC showing the SM expectation (purple shading with solid outline), and the distributions with  $\bar{c}_W = 0.1$  and  $0.05$ , respectively as red-dotted and blue-dashed lines [34]. Lower panel: The same-flavour  $p_T$  distribution of the leading lepton in a TGC analysis. The Standard Model distribution is shaded blue with solid lines, and the distribution for  $\bar{c}_{HW} = 0.1$  is shaded green with dashed lines. In both cases the last (overflow) bin provides important extra information in addition to the overall normalisation [33].

Fig. 14 [33] shows a global fit to the Higgs data, including associated production kinematics, and LHC TGC measurements. The individual 95% CL constraints with one non-zero EFT coefficient at a time are shown as green bars. The other lines show marginalised 95% ranges found using the Higgs signal-strength data in conjunction with the kinematic distributions for associated  $H + V$  production measured by ATLAS and D0 (blue bars), with the LHC TGC data (red lines), and with both (black bars). The LHC TGC constraints are the most important for  $\bar{c}_W$  and  $\bar{c}_{3W}$ , whereas the Higgs constraints are more important for  $\bar{c}_{HW}$ ,  $\bar{c}_{HB}$  and  $\bar{c}_g$ .

In my view, the EFT approach is the most promising framework for analysing Run 2 results, in particular because it can be used to tie together many different classes of measurements.

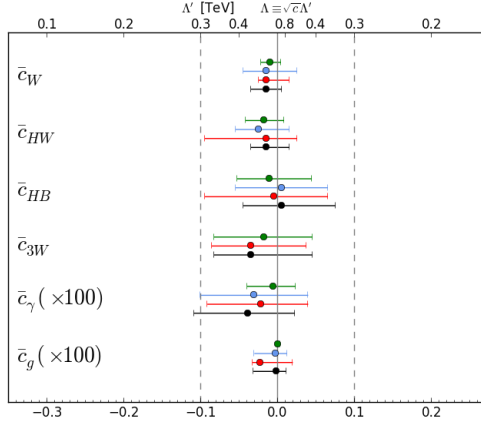


Figure 14: The 95% CL constraints for single-coefficient fits (green bars), and the marginalised 95% ranges for the LHC Higgs signal-strength data combined with the kinematic distributions for associated  $H + V$  production measured by ATLAS and D0 (blue bars), with the LHC TGC data (red lines), and the global combination with both the associated production and TGC data (black bars). Note that  $\bar{c}_{\gamma,g}$  are shown  $\times 100$ , for which the upper axis should be read  $\times 10$  [33].

## 5. The SM is not enough!

“The more important fundamental laws and facts of physical science have all been discovered” said Albert Michelson in 1894, just before radioactivity and the electron were discovered. “There is nothing new to be discovered in physics now, all that remains is more and more precise measurement” said Lord Kelvin in 1900, just before Einstein’s *annus mirabilis* in 1905. Similarly, today there are many reasons to expect physics beyond the SM even (particularly after the discovery of a (the?) Higgs boson, as I now discuss.

As James Bond might have said [35], there are 007 important reasons. 1) The measured values of  $m_t$  and  $m_H$  indicate that the electroweak vacuum is *probably* unstable, in the absence of some BSM physics. 2) The dark matter required by astrophysics and cosmology has no possible origin within the SM. 3) The origin of the matter in the Universe requires additional CP violation beyond CKM. 4) The small neutrino masses seem to require BSM physics. 5) The hierarchy of mass scales could appear more natural in the presence of some new physics at the TeV scale. 6) Cosmological inflation requires BSM physics, since the effective Higgs potential in the SM would seem to become negative at high scales. 7) Quantising gravity would certainly require physics (far) beyond the SM.

The first two of these issues are discussed in the following.

## 6. The Instability of the Electroweak Vacuum

In the SM with its  $SU(2) \times U(1)$  symmetry, the origin where  $\langle H \rangle = 0$  is unstable and surrounded by a valley where  $\langle H \rangle \equiv v = 246$  GeV, the present electroweak vacuum. At larger Higgs field values, the effective potential rises, at least for a while. However, calculations in the SM show that, for the measured values of  $m_t$  and  $m_H$ , the effective potential turns down as a result of renormalization of the Higgs self-coupling by the top quark, which overwhelms that by the Higgs itself. Thus, the present electroweak vacuum is in principle unstable in the SM, and quantum tunnelling generates collapse into an anti-de-Sitter ‘Big Crunch’.

The SM calculations [19] shown in the upper panel of Fig. 15 indicate that the instability sets in at a Higgs scale  $\Lambda$ :

$$\begin{aligned} \log_{10} \left( \frac{\Lambda}{\text{GeV}} \right) &= 11.3 + 1.0 \left( \frac{m_H}{\text{GeV}} - 125.66 \right) \\ &- 1.2 \left( \frac{m_t}{\text{GeV}} - 173.10 \right) \\ &+ 0.4 \left( \frac{\alpha_s(M_Z) - 0.1184}{0.0007} \right). \end{aligned} \quad (12)$$

Using the world average values of  $m_t$ ,  $m_H$  and  $\alpha_s(M_Z)$ , this formula yields

$$\Lambda = 10^{10.5 \pm 1.1} \text{ GeV}. \quad (13)$$

However, we see in the lower panel of Fig. 15 that this calculation is very sensitive to  $m_t$ . Note in this connection that the D0 Collaboration has recently reported a new, higher, value of  $m_t$  [36] (tending to make the vacuum more unstable), whereas the CMS Collaboration has reported lower values of  $m_t$  from new analyses [37] (tending to make the vacuum more stable). A more accurate experimental measurement of  $m_t$  would help us understand the fate of the Universe within the SM, and the possible need for BSM physics to stabilise the electroweak vacuum, but we also need to understand better the relationship between the parameter  $m_t$  in the SM Lagrangian and the effective mass parameter measured by experiments [38].

Even if the lifetime of the electroweak vacuum is much longer than the age of the Universe, as suggested by these calculations, one cannot simply ignore this problem. The early Universe is thought to have had a very high energy density, e.g., during an inflationary epoch [39], at which time quantum and thermal fluctuations at that time would have populated the anti-de-Sitter ‘Big Crunch’ region [40]. However, it is possible that we might have been lucky enough to live in a non-anti-de-Sitter region and thereby surviving [41]. The

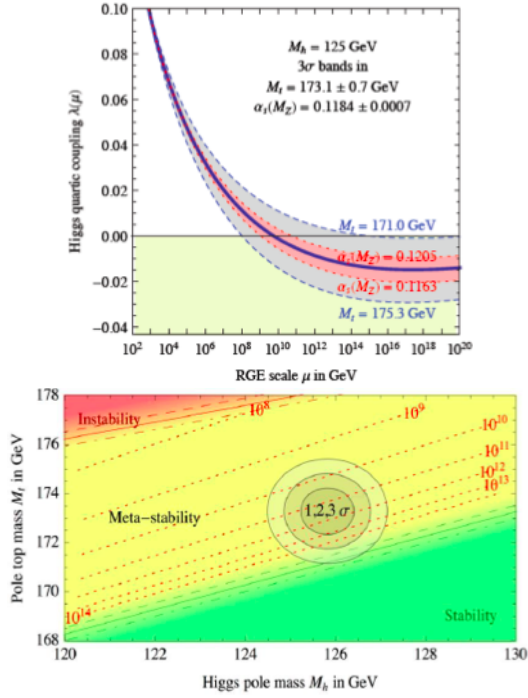


Figure 15: Left panel: Within the SM, normalisation by the top quark appears to drive the Higgs self-coupling  $\lambda < 0$  at large scales, destabilising the electroweak vacuum. Right panel: Regions of vacuum stability, metastability and instability in the  $(m_H, m_t)$  plane. Both panels are from [19].

problem could be avoided with suitable new physics beyond the SM, of which one example is supersymmetry [42].

## 7. Supersymmetry

One may love supersymmetry (SUSY) for many reasons, such as rendering the hierarchy problem more natural, providing a candidate for the cold dark matter, aiding grand unification and its essential (?) rôle in string theory. In my mind, Run 1 of the LHC has added three more reasons, namely the mass of the Higgs boson, which was predicted successfully by supersymmetry [18, 43], the fact that the Higgs couplings are similar to those of the SM Higgs boson, as discussed earlier and as expected in simple realisations of the MSSM [44], and the stabilisation of the electroweak vacuum, as mentioned just above. How can we resist SUSY's manifold charms?

However, so far SUSY has kept coyly out of sight in searches at the LHC, direct searches for the scattering of dark matter particles, indirect searches in flavour physics, etc.. Where could SUSY be hiding? We know

that SUSY must be a broken symmetry, but we do not know how, so we do not know what the SUSY spectrum may be. It is often assumed that there is a discrete R-symmetry, which would guarantee the stability of the lightest supersymmetric particle (LSP), providing the above-mentioned dark matter candidate. It is often assumed that the SUSY-breaking sparticle masses are universal at some high renormalisation scale, usually the GUT scale, but this has no strong theoretical justification. The simplest model is one in which all the SUSY-breaking contributions  $m_0$  to the squark, slepton and Higgs masses are equal at the GUT scale, and the SU(3), SU(2) and U(1) gauging masses  $m_{1/2}$  are also universal, which is called the constrained MSSM (CMSSM). It could also be that the SUSY-breaking contributions to the masses of the two Higgs doublets of the MSSM differ from those of the squarks and leptons, and may be equal to each other (the NUHM1), or different from each other (the NUHM2). Alternatively, one may consider the phenomenological MSSM (pMSSM) in which no GUT-scale universality is assumed.

Some results of global fits to the CMSSM, NUHM1, NUHM2 and a version of the pMSSM with 10 free SUSY-breaking parameters, combining all experimental and phenomenological constraints and requiring that the relic supersymmetric particle density be within the cosmological range, are shown in Fig. 16 [45, 46, 47]. The upper panel shows the profile likelihood functions for the gluino mass in these models, and the lower panel shows the likelihood functions for the first- and second-generation squarks (which are assumed to be equal in the pMSSM10). In the GUT-universal models the 95% CL lower limits on the squark and gluino masses are  $\sim 1.5$  GeV, whereas they could be significantly lighter in the pMSSM10, which offers greater prospects for discovering SUSY in LHC Run 2 [47].

The pMSSM revives the possibility of explaining the discrepancy between the SM calculation of  $g_\mu - 2$  and the experimental measurement within a SUSY model. This is not possible in the CMSSM, NUHM1 and NUHM2, because of the LHC constraints, and these models predict values of the  $g_\mu - 2$  similar to the SM prediction, as shown by the blue lines in Fig. 17. However, the black line in this Figure shows that the experimental measurement could be accommodated within the pMSSM [47]. There are plans for two new experiments to measure  $g_\mu - 2$  [49], and other low-energy  $e^+e^-$  experiments will help clarify the discrepancy between the SM and experiment.

If this is indeed due to SUSY, our pMSSM10 analysis suggests that its discovery may not be far away! In particular, there are prospects in searches for jets + missing



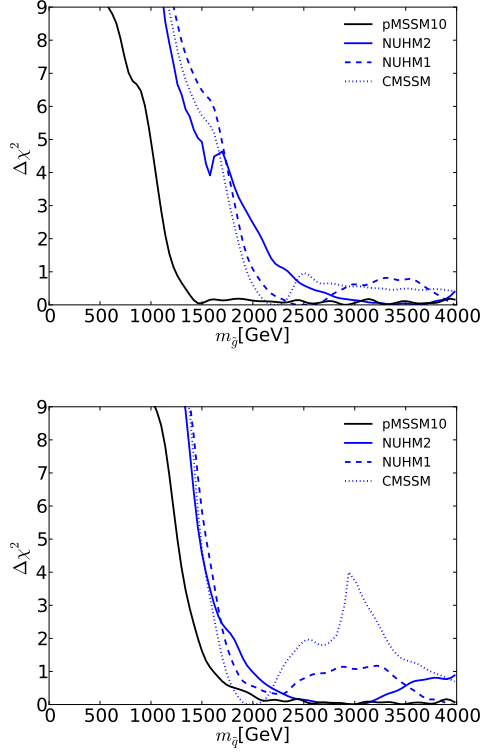


Figure 16: The profile likelihood functions for the gluino mass (upper panel) and the first- and second-generation squark masses (lower panel). The solid black lines are for the pMSSM10 [47], the solid blue lines for the NUHM2 [46], the dashed blue lines for the NUHM1 and the dotted blue lines for the CMSSM [45].

transverse energy searches at the LHC, as well as dedicated searches for sleptons and light stop squarks [47].

## 8. Dark Matter Searches

As already mentioned, a supersymmetric model that conserves R-parity has a natural candidate for a cold dark matter particle, and this is often taken to be the lightest neutralino  $\tilde{\chi}_0^1$  [50] (though other candidates are also possible). The present limits from direct searches for the scattering of massive cold dark matter particles in underground experiments are shown in the upper panel of Fig. 18, together with predictions in the pMSSM10 [47]. The 68% CL region in this model (outlined by the red contour) lies just below the current experimental limit and within range of the planned LZ experiment (magenta line) [51].

Other TeV-scale extensions of the SM, such as some extra-dimensional models with K-parity and little Higgs models with T-parity, also have possible candidates. It

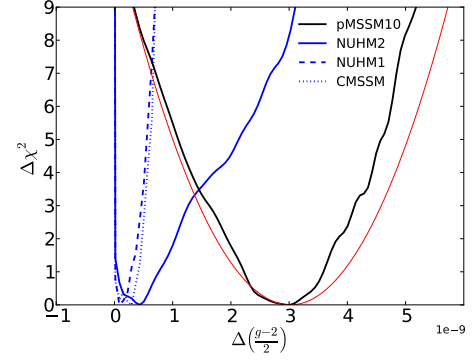


Figure 17: The one-dimensional  $\chi^2$  likelihood function for  $g_\mu - 2$  in the CMSSM, NUHM1, NUHM2 (blue lines) and the pMSSM10 (black line) [47]. The red line represents the uncertainty in the experimental range of  $g_\mu - 2$ .

is therefore useful to make a model-independent comparison of the capabilities of the LHC and direct dark matter searches, and one such is shown in the lower panel of Fig. 18. This compares direct astrophysical searches for the scattering of generic TeV-scale dark matter particles with the current reaches of the LHC via monojet searches, for the cases of spin-dependent (axial) couplings (left panel) and spin-independent (vector) couplings (right panel) [52]. In the former case the LHC monojet searches generally have greater sensitivity than the direct searches, except for dark matter particle masses  $\gtrsim 1$  TeV where the LHC runs out of phase space. On the other hand, direct searches for spin-independent interactions are more sensitive than the LHC searches for masses  $\gtrsim 4$  GeV. SUSY models generally favour a relatively large mass for the dark matter particle, the pMSSM10 being one example, as seen in the upper panel of Fig. 18.

## 9. Possible Future Colliders

There is longstanding interest in building a high-energy  $e^+e^-$  collider, which might be linear such as the ILC ( $E_{CM} \lesssim 1$  TeV) or CLIC ( $E_{CM} \lesssim 3$  TeV). On the other hand, there is now interest in Europe and China in a possible large circular tunnel to contain an  $e^+e^-$  collider with  $E_{CM} \lesssim 350$  GeV and/or a  $pp$  collider with  $E_{CM} \lesssim 100$  TeV [53]. A circular  $e^+e^-$  collider would provide measurements of the Z and Higgs bosons of unparalleled accuracy, as seen in Fig. 19 [54]. These would be able to distinguish between the predictions of the SM and various fits in the CMSSM, NUHM1 and NUHM2, as shown, if one can also reduce correspond-

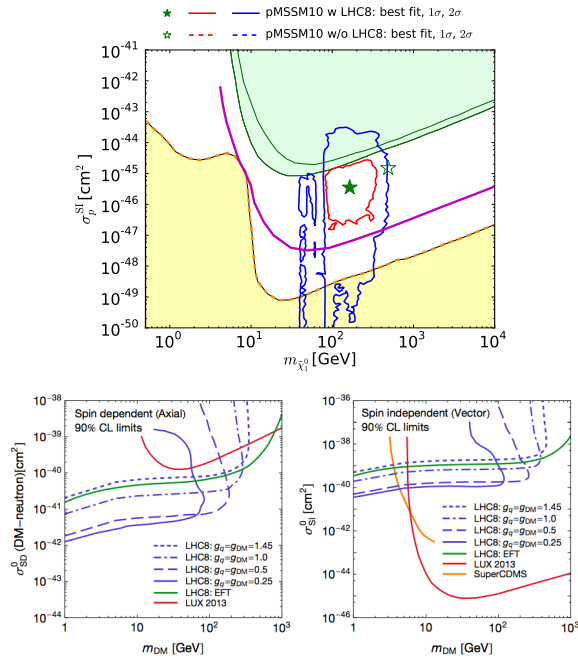


Figure 18: Upper panel: The two-dimensional profile likelihood function in the  $(m_{\tilde{\chi}_0}, \sigma_p^{SI})$ -plane [47], showing the regions excluded by the XENON100 and LUX experiments (shaded green), the neutrino ‘floor’ (shaded yellow), and the prospective sensitivity of the LZ experiment [51]. The preferred 68% CL region is outlined in red, and the region allowed at the 95% CL is outlined in blue. The solid contours incorporate the LHC constraints, and the dashed contours omit them. Lower panels: A comparison of the current 90% CL direct search limits from LUX and SuperCDMS (red and orange lines, respectively), the monojet limits in simple models (blue lines) and the limits in an effective field theory framework (green line) in the cross section vs  $m_{DM}$  plane used by the direct detection community. The left and right panels show, respectively, the limits on the spin-dependent and spin-independent cross sections appropriate for axial- vector and vector mediators [52].

ingly the present theoretical uncertainties, which are indicated in the right panel by the shaded green bars. The other coloured bars illustrate the accuracies attainable with measurements at various accelerators.

A future high-energy  $pp$  collider would produce many more Higgs bosons than the LHC, as seen in the upper panel of Fig. 20 [55], offering the possibility of measuring Higgs couplings with greater statistical accuracy, and also including the elusive triple-Higgs coupling. A high-energy  $pp$  collider would also offer unique possibilities to discover and/or measure the properties of SUSY particles. Even the SUSY dark matter particle could weigh several TeV, as seen in the lower panel of Fig. 20 [56], which illustrates a strip in the CMSSM parameter space where the relic neutralino density is brought into the the range allowed by cosmol-

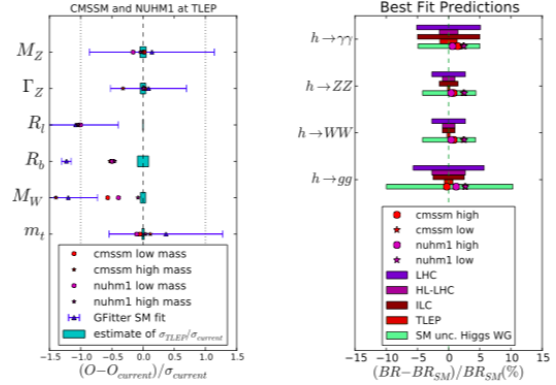


Figure 19: Comparison of the present precisions in measurements of various Z properties (left panel) and Higgs couplings (right panel), together with the prospective precisions of possible measurements at future colliders and the deviations from the SM predictions found at the best-fit points in various SUSY models. The right panel also shows the current theoretical uncertainties. From [54].

ogy through coannihilation with the lighter stop squark. In the example shown, the lightest neutralino weighs  $\lesssim 3$  TeV and only a  $pp$  collider with  $E_{CM} \sim 100$  TeV would be able to explore all the range of particle masses compatible with SUSY providing dark matter (solid and upper dashed blue lines). For all this range calculations of the Higgs mass are compatible with the experimental value (represented by the yellow band), considering the theoretical uncertainties represented by the solid and dashed green lines.

The supersymmetric dark matter particle might be even heavier in more general supersymmetric models. For example, if the lightest neutralino coannihilates with an almost degenerate gluino, it may weigh  $\lesssim 8$  TeV, as seen in Fig. 21, which would be a challenge even for a 100-TeV collider.

The physics cases for future large circular colliders are still being explored. There will be bread-and-butter high-precision Higgs and other SM measurements to probe possible BSM scenarios for physics. As for direct searches for new physics, the search for dark matter particles may provide the strongest case, and this is under continuing study.

## 10. Conclusion

The physics landscape will look completely different when/if future runs of the LHC find evidence for new physics beyond the SM such as SUSY. The LHC adventure has only just begun, and we look forward to a big increase in energy with Run 2 and eventually two orders of magnitude more integrated luminosity. Lovers

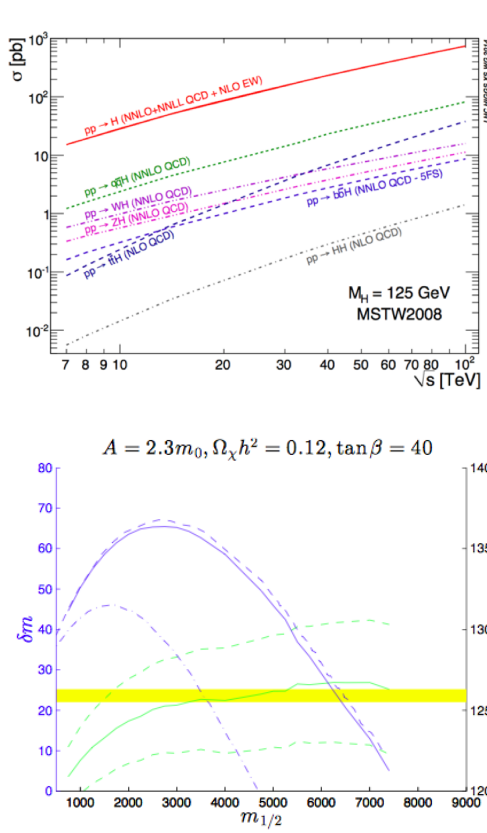


Figure 20: Upper panel: Cross sections for various Higgs production processes at pp colliders as functions of the centre-of-mass energy [55]. Lower panel: One of the possibilities for a relatively heavy SUSY dark matter particle weighing  $\sim 0.4m_{1/2} \lesssim 3$  TeV. The vertical axis is the mass difference between the dark matter particle and the next-to-lightest supersymmetric particle, in this case the lighter stop squark. The solid and upper dashed blue lines correspond to the current central and  $+1\sigma$  values of the dark matter density, the horizontal yellow band represents the experimental value of the Higgs mass, and the green solid and dashed lines represent the central value and  $\pm 1\sigma$  uncertainties in theoretical calculations of the Higgs mass [56].

of SUSY should not be disappointed that she has not yet appeared. It took 48 years for the Higgs boson to be discovered, but four-dimensional SUSY models were first written down just 41 years ago [58]. We can be patient for a while longer.

## Acknowledgements

The author is supported in part by the London Centre for Terauniverse Studies (LCTS), using funding from the European Research Council via the Advanced Investigator Grant 267352, and in part by STFC (UK) via the research grants ST/J002798/1 and ST/L000326/1.

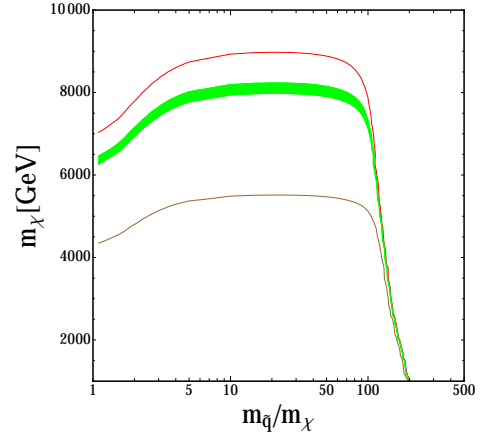


Figure 21: The mass of the dark matter particle (assumed to be a Bino) at the endpoint of the gluino coannihilation strip when  $\Delta m = m_{\tilde{g}} - m_\chi = 0$ , as a function of  $m_q/m_\chi$ . The green band corresponds to the current  $3\sigma$  range of the dark matter density:  $\Omega_\chi h^2 = 0.1193 \pm 0.0042$ , and the brown and red contours are for  $\Omega_\chi h^2 = 0.05$  and  $0.15$ , respectively. From [57].

## References

- [1] CMS Collaboration, <https://twiki.cern.ch/twiki/bin/view/CMSPublic/PhysicsResultsSMP>.
- [2] G. Aad *et al.* [ATLAS Collaboration], Phys. Lett. B **716** (2012) 1 [arXiv:1207.7214 [hep-ex]]; S. Chatrchyan *et al.* [CMS Collaboration], Phys. Lett. B **716** (2012) 30 [arXiv:1207.7235 [hep-ex]].
- [3] V. Khachatryan *et al.* [CMS Collaboration], arXiv:1410.6765 [hep-ex].
- [4] A. David *et al.* [LHC Higgs Cross Section Working Group Collaboration], arXiv:1209.0040 [hep-ph].
- [5] C. Anastasiou, C. Duhr, F. Dulat, F. Herzog and B. Mistlberger, arXiv:1503.06056 [hep-ph].
- [6] J. Charles, O. Deschamps, S. Descotes-Genon, H. Lacker, A. Menzel, S. Monteil, V. Niess and J. Ocariz *et al.*, arXiv:1501.05013 [hep-ph].
- [7] V. Khachatryan *et al.* [CMS and LHCb Collaborations], arXiv:1411.4413 [hep-ex] and references therein.
- [8] R. Aaij *et al.* [LHCb Collaboration], Phys. Rev. Lett. **113** (2014) 151601 [arXiv:1406.6482 [hep-ex]].
- [9] R. Aaij *et al.* [LHCb Collaboration], Phys. Rev. Lett. **111** (2013) 19, 191801 [arXiv:1308.1707 [hep-ex]].
- [10] V. Khachatryan *et al.* [CMS Collaboration], arXiv:1502.07400 [hep-ex].
- [11] V. M. Abazov *et al.* [D0 Collaboration], Phys. Rev. Lett. **105** (2010) 081801 [arXiv:1007.0395 [hep-ex]].
- [12] B. Kronenbitter *et al.* [Belle Collaboration], arXiv:1503.05613 [hep-ex].
- [13] T. Aaltonen *et al.* [CDF Collaboration], Phys. Rev. D **87** (2013) 9, 092002 [arXiv:1211.1003 [hep-ex]].
- [14] S. J. Brodsky and X. G. Wu, Phys. Rev. D **85** (2012) 114040 [arXiv:1205.1232 [hep-ph]]; S. Q. Wang, X. G. Wu, Z. G. Si and S. J. Brodsky, Phys. Rev. D **90** (2014) 11, 114034 [arXiv:1410.1607 [hep-ph]].
- [15] G. Aad *et al.* [ATLAS Collaboration], Phys. Rev. D **90** (2014) 052004 [arXiv:1406.3827 [hep-ex]].

- [16] V. Khachatryan *et al.* [CMS Collaboration], arXiv:1412.8662 [hep-ex].
- [17] G. Aad *et al.* [ATLAS and CMS Collaborations], arXiv:1503.07589 [hep-ex].
- [18] J. R. Ellis, G. Ridolfi and F. Zwirner, Phys. Lett. B **257** (1991) 83; H. E. Haber and R. Hempfling, Phys. Rev. Lett. **66** (1991) 1815; Y. Okada, M. Yamaguchi and T. Yanagida, Prog. Theor. Phys. **85** (1991) 1.
- [19] D. Buttazzo, G. Degrandi, P. P. Giardino, G. F. Giudice, F. Sala, A. Salvio and A. Strumia, JHEP **1312** (2013) 089 [arXiv:1307.3536].
- [20] G. Aad *et al.* [ATLAS Collaboration], Phys. Lett. B **726** (2013) 120 [arXiv:1307.1432 [hep-ex]].
- [21] V. Khachatryan *et al.* [CMS Collaboration], arXiv:1411.3441 [hep-ex].
- [22] T. Aaltonen *et al.* [CDF and D0 Collaborations], arXiv:1502.00967 [hep-ex].
- [23] J. Ellis, V. Sanz and T. You, Phys. Lett. B **726** (2013) 244 [arXiv:1211.3068 [hep-ph]].
- [24] J. Ellis, D. S. Hwang, V. Sanz and T. You, JHEP **1211** (2012) 134 [arXiv:1208.6002 [hep-ph]].
- [25] J. Ellis, R. Fok, D. S. Hwang, V. Sanz and T. You, Eur. Phys. J. C **73** (2013) 2488 [arXiv:1210.5229 [hep-ph]], and references therein.
- [26] ATLAS Collaboration, <https://twiki.cern.ch/twiki/bin/view/AtlasPublic/HiggsPublicResults>.
- [27] S. Chatrchyan *et al.* [CMS Collaboration], JHEP **1306** (2013) 081 [arXiv:1303.4571 [hep-ex]].
- [28] CDF and D0 Collaborations, <http://tevnphwg.fnal.gov>.
- [29] J. Ellis and T. You, JHEP **1306** (2013) 103 [arXiv:1303.3879 [hep-ph]]. References to the original literature can be found here.
- [30] G. Blankenburg, J. Ellis and G. Isidori, Phys. Lett. B **712** (2012) 386 [arXiv:1202.5704 [hep-ph]].
- [31] A. Askew, P. Jaiswal, T. Okui, H. B. Prosper and N. Sato, arXiv:1501.03156 [hep-ph].
- [32] J. Ellis, D. S. Hwang, K. Sakurai and M. Takeuchi, JHEP **1404** (2014) 004 [arXiv:1312.5736 [hep-ph]].
- [33] J. Ellis, V. Sanz and T. You, arXiv:1410.7703 [hep-ph]. References to the original literature can be found here.
- [34] J. Ellis, V. Sanz and T. You, JHEP **1407** (2014) 036 [arXiv:1404.3667 [hep-ph]].
- [35] J. Bond *et al.*, <http://www.imdb.com/title/tt0143145/>.
- [36] A. Jung, on behalf of the D0 Collaboration, <https://indico.cern.ch/event/279518/session/27/contribution/36/material/slides/0.pdf>.
- [37] CMS Collaboration, <http://cds.cern.ch/record/1951019/files/T0P-14-015-pas.pdf>.
- [38] S. Moch, S. Weinzierl, S. Alekhin, J. Blumlein, L. de la Cruz, S. Dittmaier, M. Dowling and J. Erler *et al.*, arXiv:1405.4781 [hep-ph].
- [39] P. A. R. Ade *et al.* [BICEP2 and Planck Collaborations], Phys. Rev. Lett. **114** (2015) 10, 101301 [arXiv:1502.00612 [astro-ph.CO]]; P. A. R. Ade *et al.* [Planck Collaboration], arXiv:1502.02114 [astro-ph.CO].
- [40] M. Fairbairn and R. Hogan, Phys. Rev. Lett. **112** (2014) 201801 [arXiv:1403.6786 [hep-ph]].
- [41] A. Hook, J. Kearney, B. Shakya and K. M. Zurek, arXiv:1404.5953 [hep-ph]; J. Kearney, H. Yoo and K. M. Zurek, arXiv:1503.05193 [hep-th].
- [42] J. R. Ellis and D. Ross, Phys. Lett. B **506** (2001) 331 [hep-ph/0012067].
- [43] T. Hahn, S. Heinemeyer, W. Hollik, H. Rzehak and G. Weiglein, Phys. Rev. Lett. **112** (2014) 14, 141801 [arXiv:1312.4937 [hep-ph]].
- [44] J. R. Ellis, S. Heinemeyer, K. A. Olive and G. Weiglein, Phys. Lett. B **515** (2001) 348 [hep-ph/0105061].
- [45] O. Buchmueller, R. Cavanaugh, A. De Roeck, M. J. Dolan, J. R. Ellis, H. Flacher, S. Heinemeyer and G. Isidori *et al.*, Eur. Phys. J. C **74** (2014) 6, 2922 [arXiv:1312.5250 [hep-ph]].
- [46] O. Buchmueller, R. Cavanaugh, M. Citron, A. De Roeck, M. J. Dolan, J. R. Ellis, H. Flacher and S. Heinemeyer *et al.*, arXiv:1408.4060 [hep-ph].
- [47]
- [48] K. J. de Vries, E. A. Bagnaschi, O. Buchmueller, R. Cavanaugh, M. Citron, A. De Roeck, M. J. Dolan and J. R. Ellis *et al.*, arXiv:1504.03260 [hep-ph].
- [49] FNAL g-2 Collaboration, <http://muon-g-2.fnal.gov>; H. Iinuma (for the J-PARC New g-2/EDM experiment Collaboration), [http://iopscience.iop.org/1742-6596/295/1/012032/pdf/1742-6596\\_295\\_1\\_012032.pdf](http://iopscience.iop.org/1742-6596/295/1/012032/pdf/1742-6596_295_1_012032.pdf).
- [50] J. R. Ellis, J. S. Hagelin, D. V. Nanopoulos, K. A. Olive and M. Srednicki, Nucl. Phys. B **238** (1984) 453; H. Goldberg, Phys. Rev. Lett. **50** (1983) 1419 [Erratum-ibid. **103** (2009) 099905].
- [51] P. Cushman, C. Galbiati, D. N. McKinsey, H. Robertson, T. M. P. Tait, D. Bauer, A. Borgland and B. Cabrera *et al.*, arXiv:1310.8327 [hep-ex].
- [52] O. Buchmueller, M. J. Dolan, S. A. Malik and C. McCabe, JHEP **1501** (2015) 037 [arXiv:1407.8257 [hep-ph]]; S. Malik, C. McCabe, H. Araujo, A. Belyaev, C. Boehm, J. Brooke, O. Buchmueller and G. Davies *et al.*, arXiv:1409.4075 [hep-ex].
- [53] <https://espace2013.cern.ch/fcc/Pages/default.aspx>.
- [54] M. Bicer *et al.* [TLEP Design Study Working Group Collaboration], JHEP **1401** (2014) 164 [arXiv:1308.6176 [hep-ex]].
- [55] LHC Higgs Cross-Section Working Group, as reported in M. Klute, <http://indico.cern.ch/event/300048/session/13/contribution/60/material/slides/0.pdf>.
- [56] J. Ellis, K. A. Olive and J. Zheng, Eur. Phys. J. C **74** (2014) 2947 [arXiv:1404.5571 [hep-ph]].
- [57] J. Ellis, F. Luo and K. A. Olive, arXiv:1503.07142 [hep-ph].
- [58] J. Wess and B. Zumino, Phys. Lett. B **49** (1974) 52.